Tailoring Josephson Coupling through Superconductivity-Induced Nonequilibrium

F. Giazotto,[1,*] T. T. Heikkilä,[2] F. Taddei,[1] Rosario Fazio,[1] J. P. Pekola,[2] and F. Beltram[1]

[1]*NEST-INFM & Scuola Normale Superiore, I-56126 Pisa, Italy*
[2]*Low Temperature Laboratory, Helsinki University of Technology, P.O. Box 2200, FIN-02015 HUT, Finland*
(Received 14 November 2003; published 29 March 2004)

The distinctive quasiparticle distribution existing under nonequilibrium in a superconductor-insulator-normal metal-insulator-superconductor mesoscopic line is proposed as a novel tool to control the supercurrent intensity in a long Josephson weak link. We present a description of this system in the framework of the diffusive-limit quasiclassical Green-function theory and take into account the effects of inelastic scattering with arbitrary strength. Supercurrent enhancement and suppression, including a marked transition to a π junction, are striking features leading to a fully tunable structure.

Nonequilibrium effects in mesoscopic superconducting circuits have been receiving rekindled attention during the last few years [1]. The art of controlling Josephson coupling in superconductor-normal metal-superconductor (SNS) weak links is at present in the spotlight: a recent breakthrough in mesoscopic superconductivity is indeed represented by the SNS transistor, where supercurrent suppression as well as its sign reversal (π transition) were demonstrated [2,3]. This was achieved by driving the quasiparticle distribution in the weak link far from equilibrium [4–6] through external voltage terminals, viz., normal reservoirs. Such behavior relies on the two-step shape of the quasiparticle nonequilibrium distribution, typical of diffusive mesoscopic wires and experimentally observed by Pothier and coworkers [7].

The purpose of this Letter is to demonstrate that it is possible to tailor the quasiparticle distribution through *superconductivity-induced* nonequilibrium in order to implement a unique class of superconducting transistors. This can be achieved when mesoscopic control lines are connected to superconducting reservoirs through tunnel barriers (*I*), realizing a superconductor-insulator-normal metal-insulator-superconductor (SINIS) channel. The peculiar quasiparticle distribution in the *N* region, originating from biasing the *S* terminals, allows one to access several regimes, from supercurrent enhancement with respect to equilibrium to a large amplitude of the π transition passing through a steep supercurrent suppression. These features are accompanied by a large current gain (up to some 10^5 in the region of larger input impedance) and reduced dissipation. The ultimate operating frequencies available open the way to the exploitation of this scheme for the implementation of ultrafast current amplifiers.

The investigated mesoscopic structure (see Fig. 1) consists of a long diffusive weak link of length L_J much larger than the superconducting coherence length (ξ_0) oriented along the *x* direction. This defines the SNS junction of cross section A_J. The superconducting terminals belonging to the SNS junction, labeled S_J (3 and 4),

are kept at zero potential. The SINIS control line is oriented along the *y* direction and consists of a normal wire, of length L_C and cross section A_C, connected through identical tunnel junctions of resistance $\mathcal{R}_T$ to two superconducting reservoirs S_C (1 and 2), biased at opposite voltages $\pm V_C/2$. The superconducting gaps of S_J and S_C (Δ_J and Δ_C) are in general different.

The supercurrent I_J flowing across the SNS junction is given by [5,6]

$$I_J(V_C) = \frac{\sigma A_J}{eL_J} \int_0^\infty dE\,[f(-E;V_C) - f(E;V_C)]\mathrm{Im}[j_E], \quad (1)$$

and depends on the quasiparticle distribution function $f(E)$. In Eq. (1), σ is the normal-state conductivity which determines the normal-state resistance of the junction according to $R_N = L_J/\sigma A_J$. The distribution function f reduces to the equilibrium Fermi distribution when $V_C = 0$. The energy-dependent spectral supercurrent [8,9], $\mathrm{Im}[j_E]$, can be calculated by solving the Usadel equations [10]. Following the parametrization of the Green functions given in Ref. [8], these equations in the *N* region can be written
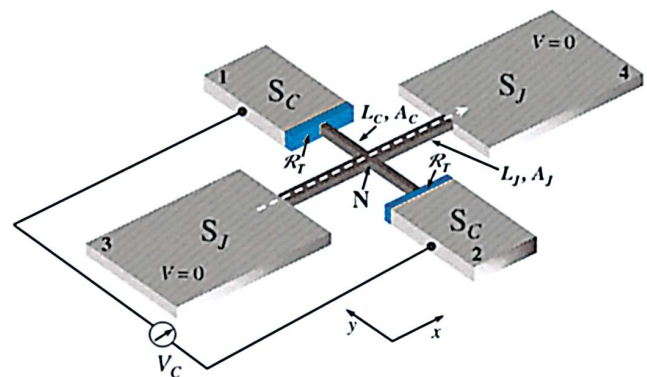

FIG. 1 (color). Scheme of the Josephson transistor. The supercurrent I_J (along the white dashed line) is tuned by applying a bias V_C across the SINIS symmetric line connected to the center of the weak link. All normal wires are assumed quasi-one-dimensional.

$$j_E = -\sinh^2(\theta)\partial_x\chi, \qquad \partial_x j_E = 0,$$

$$\hbar D \partial_x^2 \theta + 2iE\sinh\theta - \frac{\hbar D}{2}(\partial_x\chi)^2 \sinh(2\theta) = 0, \qquad (2)$$

where D is the diffusion coefficient and E is the energy relative to the chemical potential in S_J. $\theta(x,E)$ and $\chi(x,E)$ are in general complex functions. For perfectly transmissive contacts, the boundary conditions at the S_JN interfaces reduce to $\theta = \text{arctanh}(\Delta_J/E)$ and $\chi = \pm\phi/2$ in the reservoirs S_J, where ϕ is the phase difference between the superconductors.

As required by Eq. (1), we must determine the actual quasiparticle distribution in the N region of the SINIS structure. This is controlled by voltage (V_C) and temperature and by the amount of inelastic scattering in the control line. In the case of a short control wire with no inelastic interactions, the quasiparticle distribution, according to Ref. [11], is given by

$$f(E,V_C) = \frac{\mathcal{N}_1 \mathcal{F}_1 + \mathcal{N}_2 \mathcal{F}_2}{\mathcal{N}_1 + \mathcal{N}_2}, \qquad (3)$$

where $\mathcal{N}_{1,2} = \mathcal{N}_{S_C}(E \pm eV_C/2)$ and $\mathcal{F}_{1,2} = \mathcal{F}^0(E \pm eV_C/2)$. The former are the BCS densities of states in the reservoirs S_C (labeled 1 and 2 in Fig. 1). $\mathcal{F}^0(E)$ is the Fermi function at lattice temperature T [12]. In this case Eqs. (1) and (3) yield the dimensionless transistor output characteristics shown in Fig. 2(a). The latter plots the supercurrent I_J vs control bias V_C at different temperatures for a long junction (i.e., $\Delta_J \gg E_{\text{Th}}^J$, where $E_{\text{Th}}^J = \hbar D/L_J^2$ is the Thouless energy of the SNS junction, as this is the limit where the supercurrent spectrum varies strongly with energy). We assumed $\phi = \pi/2$, $T_c^C/T_c^J = 0.2$, where $T_c^{C(J)}$ are the critical temperatures of the superconductors $S_{C(J)}$ and L_J such that $\Delta_J/E_{\text{Th}}^J = 300$.

At the lowest temperatures, increasing V_C leads to a large supercurrent enhancement with respect to equilibrium slightly below $V_C = 2\Delta_C(T)/e = V_C^*(T)$ (region I in Fig 2). Further increase of bias leads to a π transition (region II) and finally to a decay for larger voltages [14]. This behavior is explained in Figs. 2(b)–2(d), where the spectral supercurrent (solid line) is plotted together with $f(-E) - f(E)$ (dash-dotted line) for values of V_C and T corresponding to regions I, II, and III, respectively. Hatched areas represent the integral of their product, i.e., the supercurrent I_J of Eq. (1). In particular, region I corresponds to the *cooling* regime where hot quasiparticles are extracted from the normal metal [11,15]. The origin of the π transition in region II is illustrated by Fig. 2(c), where the negative contribution to the integral is shown. We remark that the intensity of the supercurrent inversion is very significant. It reaches about 60% of the maximum value of I_J at $V_C \simeq V_C^*(T)$ in the whole temperature range, nearly doubling the π-state value of the
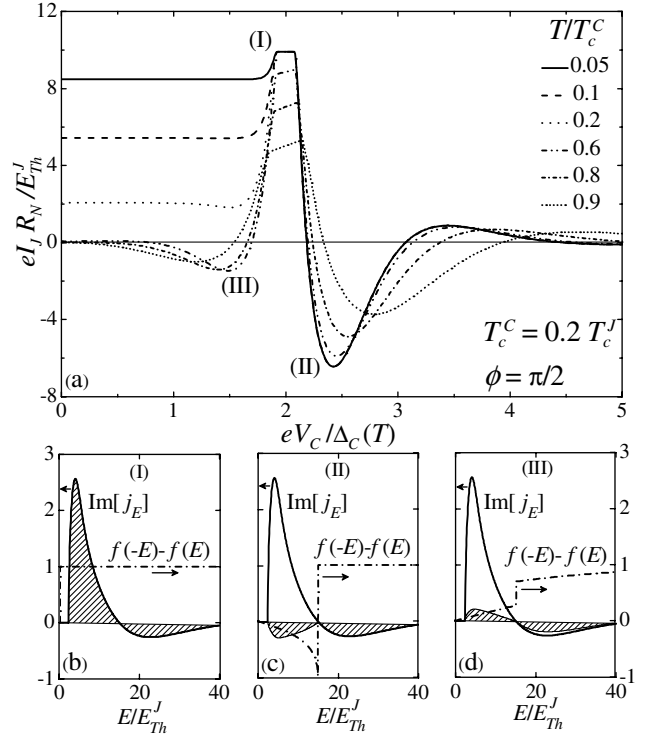

FIG. 2. (a) Supercurrent vs control voltage V_C at different temperatures (T) for $\phi = \pi/2$ and $T_c^C = 0.2\,T_c^J$ (see text). Bias regions labeled (I), (II), and (III) indicate supercurrent enhancement due to quasiparticle *cooling*, high-voltage π state and low-voltage π state in the high-temperature regime, respectively. These are qualitatively explained in (b), (c), and (d), where hatched areas represent the contribution to supercurrent arising in such bias ranges (see text).

supercurrent as compared to the case of an all-normal control channel [5,6]. In the high-temperature regime ($T/T_c^C \gtrsim 0.6$), when the equilibrium critical current is vanishing, the supercurrent first undergoes a low-bias π transition (region III in Fig. 2), then enters regions I and II. This recover of the supercurrent from vanishingly small values at equilibrium is again the consequence of the peculiar shape of f [see Fig. 2(d)]. Notably, the supercurrent enhancement around $V_C^*(T)$ remains pronounced even at the highest temperatures, so that I_J attains values largely exceeding 50% of the junction maximum supercurrent. This demonstrates the full tunability of the supercurrent through nonequilibrium effects induced by the superconducting control lines. We remark that this is a unique feature stemming from the superconductivity-induced nonequilibrium population in the weak link.

The length L_C of the SINIS control line can be additionally varied to control the supercurrent by changing the effective strength of inelastic scattering in the N region. For $\mathcal{R}_T \gg R_C = L_C/\sigma A_C$, the distribution function $f(E)$ in the N region is essentially y independent and we have

$$\frac{1}{e^2 \mathcal{R}_T \Omega_C \nu_F}\{\mathcal{N}_1[\mathcal{F}_1 - f(E)] + \mathcal{N}_2[\mathcal{F}_2 - f(E)]\} + \kappa \int d\omega d\varepsilon\, \omega^\alpha I(\omega, \varepsilon, E) = 0. \qquad (4)$$

Here ν_F is the normal-metal density of states at the Fermi energy, Ω_C is the volume of the N region, and I is the net collision rate at energy E. At low temperatures, the most relevant scattering mechanism is electron-electron scattering [16] and we can neglect the effect of electron-phonon scattering. Then [7,17],

$$\mathcal{I}(\omega, \varepsilon, E) = \mathcal{I}^{\text{in}}(\omega, \varepsilon, E) - \mathcal{I}^{\text{out}}(\omega, \varepsilon, E), \qquad (5)$$

and

$$\mathcal{I}^{\text{in}}(\omega, \varepsilon, E) = [1 - f(\varepsilon)][1 - f(E)]f(\varepsilon - \omega)f(E + \omega), \qquad (6)$$

$$\mathcal{I}^{\text{out}}(\omega, \varepsilon, E) = [1 - f(\varepsilon - \omega)][1 - f(E + \omega)]f(\varepsilon)f(E). \qquad (7)$$

Electron-electron interaction is either due to direct Coulomb scattering [18,19] or mediated by magnetic impurities [16]. Below, we concentrate on the former but the latter would yield a similar qualitative behavior. From the calculation of the screened Coulomb interaction in the diffusive channel, it follows [18] that $\alpha = -3/2$ for a quasi-one-dimensional wire and $\kappa = (\pi\sqrt{D/2}\hbar^{3/2}\nu_F A_C)^{-1}$ [19]. We note that Δ_C is the most relevant energy scale to describe the distribution function for different voltages V_C. It is thus useful to replace $\omega \rightarrow \omega/\Delta_C$ and $\varepsilon \rightarrow \varepsilon/\Delta_C$ in order to obtain a dimensionless equation. Multiplying Eq. (4) by $e^2 \mathcal{R}_T \Omega_C \nu_F$, we obtain

$$\mathcal{N}_1[\mathcal{F}_1 - f(E)] - \mathcal{N}_2[f(E) - \mathcal{F}_2] = \mathcal{K}_{\text{coll}} \int d\omega d\varepsilon \, \omega^{-3/2} I(\omega, \varepsilon, E), \qquad (8)$$

where $\mathcal{K}_{\text{coll}} = (\mathcal{R}_T/R_C)(L_C^2 \kappa/D)\sqrt{\Delta_C} = \sqrt{2}(\mathcal{R}_T/R_K) \times \sqrt{(\Delta_C/E_{\text{Th}}^C)}$, $R_K = h/2e^2$, and $E_{\text{Th}}^C = \hbar D/L_C^2$. In the absence of electron-electron interaction ($\mathcal{K}_{\text{coll}} = 0$), Eq. (3) is recovered.

The influence of inelastic scattering on I_J is shown in Fig. 3, which displays the critical current of a long junction at $T = 0.1 T_c^C$ for several values of $\mathcal{K}_{\text{coll}}$. Here I_J is obtained by numerically solving Eq. (8). The effect of electron-electron interaction is to strongly suppress the π state and to widen the peak around V_C^*. The π transition vanishes for $\mathcal{K}_{\text{coll}} \simeq 100$, but the I_J enhancement due to quasiparticle cooling still persists in the limit of even larger inelastic scattering [20]. The disappearance of the π state can be understood by looking at the right inset of Fig. 3, which clearly shows how f (calculated at $eV_C = 2.5\Delta_C$) gradually relaxes from nonequilibrium towards a Fermi function upon increasing $\mathcal{K}_{\text{coll}}$. The left inset shows how f (evaluated at $eV_C = 1.5\Delta_C$) sharpens, thus enhancing I_J, by increasing $\mathcal{K}_{\text{coll}}$. This effect follows

from the fact that inelastic interactions redistribute the occupation of quasiparticle levels in the N region, thus increasing the occupation at higher energy. As a consequence, higher-energy excitations are more effectively removed by tunneling, even for biases well below and not only around V_C^* (as in the case of $\mathcal{K}_{\text{coll}} = 0$). At the same time, supercurrent recovery at high temperature is gradually weakened upon enhancing $\mathcal{K}_{\text{coll}}$. Notably, these calculations show that a rather large amount of inelastic scattering is necessary to weaken and completely suppress the π state. For example, using $Al/Al_2O_3/Cu$ as materials composing the SINIS line, $\mathcal{K}_{\text{coll}} = 1$ corresponds to use a fairly long control line with $L_C \simeq 2.3 \, \mu m$ [21].

Changing the ratio T_c^C/T_c^J shifts the I_J response along the V_C axis, the shape of the characteristics being
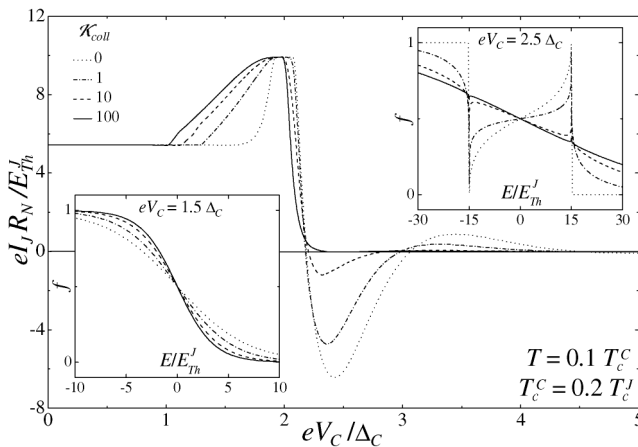

FIG. 3. Supercurrent vs V_C for various $\mathcal{K}_{\text{coll}}$ with $T = 0.1 T_c^C$ and $T_c^C = 0.2 T_c^J$. Insets show the distribution function at $eV_C = 1.5\Delta_C$ (left) and $eV_C = 2.5\Delta_C$ (right) calculated for the same $\mathcal{K}_{\text{coll}}$ values.
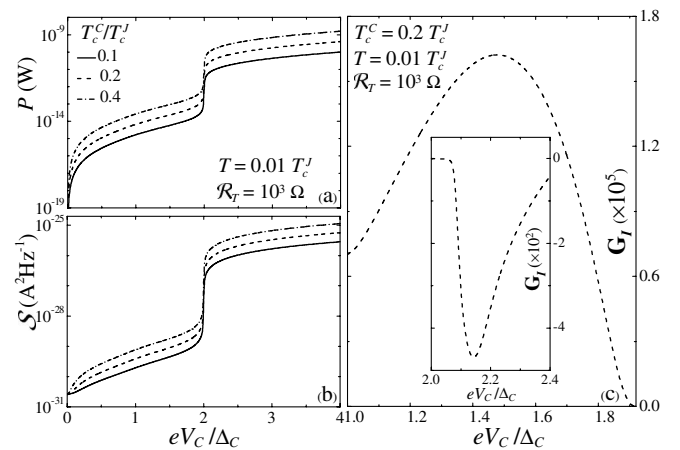

FIG. 4. (a) Power dissipated in the SINIS line vs V_C calculated for various ratios T_c^C/T_c^J and $T = 0.01 T_c^J$. (b) Noise power S vs V_C calculated for the same parameters as in (a). (c) Differential current gain $\mathbf{G}_I$ vs V_C for $T_c^C/T_c^J = 0.2$. The inset shows $\mathbf{G}_I$ in the high-bias region. In all these calculations we set $\mathcal{K}_{\text{coll}} = 0$ and $T_c^J = 9.26$ K (Nb).

virtually independent of T_c^C. This translates into a different magnitude of control voltages V_C and power dissipation $P = I_C V_C$, where I_C is the control current across the SINIS channel. The function $P(V_C)$ is plotted in Fig. 4(a) for some ratios T_c^C/T_c^J at $T = 0.01 T_c^J$, assuming $\mathcal{R}_T = 10^3 \ \Omega$ and $T_c^J = 9.26$ K. The impact of Δ_C in controlling power dissipation is easily recognized. These effects clearly indicate that $\Delta_C \ll \Delta_J$ is the condition to be fulfilled in order to minimize P. In practice, the power dissipation for $V_C > V_C^*$ constitutes an experimental problem as this energy needs to be carried out from the reservoirs. In a similar way the noise properties of the system are sensitive to the different T_c^C/T_c^J ratios. Assuming that the noise through one junction is essentially uncorrelated from the noise through the other, it follows that the input noise power S in the control line can be expressed as

$$ S = \frac{1}{\mathcal{R}_T} \int_{-\infty}^{\infty} dE \, \mathcal{N}_1 \{ f(E)(1 - \mathcal{F}_1) + \mathcal{F}_1 [1 - f(E)] \}. \tag{9} $$

$S(V_C)$ from Eq. (9) is shown in Fig. 4(b) for the same parameters of Fig. 4(a). For example, for $T_c^C/T_c^J = 0.1$ (corresponding roughly to the combination Al/Nb), P obtains values of the order of a few 10^{-15} W and S of some $10^{-30} \mathrm{A^2 \, Hz^{-1}}$ in the cooling regime, while these values are enhanced, respectively, to few tens of 10^{-12} W and $10^{-26} \mathrm{A^2 \, Hz^{-1}}$ for biases around the π transition.

In light of the possible use of this operational principle for device implementation, let us comment on the available gain and switching times. Input and output voltages are of the order of Δ_C/e and E_{Th}^J/e, respectively, so that it seems hard to achieve voltage gain. On the other hand, differential current gain $\mathbf{G}_I = dI_J/dI_C = (dI_J/dV_C) \times (dI_C/dV_C)^{-1}$ can be very large. For $V_C > V_C^*$ a simple estimate gives $\mathbf{G}_I \sim (E_{\mathrm{Th}}^J/\Delta_C)(\mathcal{R}_T/R_N)$, meaning that with realistic ratios $\mathcal{R}_T/R_N$ $(\sim 10^3)$, $\mathbf{G}_I$ can exceed 10^2. $\mathbf{G}_I(V_C)$ calculated for $T_c^C/T_c^J = 0.2$ is plotted in Fig. 4(c) (the inset shows the gain in the π-state region). This calculation reveals that $\mathbf{G}_I$ can reach huge values, with some 10^5 for $V_C < V_C^*$ [22] and several 10^2 in the opposite regime. Remarkably, gain is almost unchanged also in the presence of weak inelastic scattering (i.e., $\mathcal{K}_{\mathrm{coll}} = 1$). The same holds for P and S. As far as power gain is concerned, the Josephson junction has to be operated in the *dissipative* regime in order to get out power. An estimate for the differential power gain gives $\mathbf{G}_P = dP_J/dP \sim (E_{\mathrm{Th}}^J/\Delta_C)\mathbf{G}_I \sim 10^3 - 10^4$ for $V_C < V_C^*$ and ~ 10 for $V_C > V_C^*$. The highest operating frequency ν of the transistor is limited by the smallest energy in the system: $\nu \lesssim \min\frac{1}{h}\{\Delta_C, \Delta_J, E_{\mathrm{Th}}^C, E_{\mathrm{Th}}^J, h(\mathcal{R}_T C)^{-1}\}$, where C is the tunnel junction capacitance. For an optimized device, working frequencies of the order of 10^{11} Hz can be experimentally achieved in the high-voltage regime $V_C > V_C^*$. For $V_C < V_C^*$, conversely, the response is slower (somewhat below 10^9 Hz), owing to the long discharging time through the junctions.

*Electronic address: giazotto@sns.it
[1] See, for example, *Theory of Nonequilibrium Superconductivity*, edited by N. B. Kopnin (Clarendon Press, Oxford, 2001).
[2] J. J. A. Baselmans, A. F. Morpurgo, B. J. van Wees, and T. M. Klapwijk, Nature (London) **397**, 43 (1999); J. Huang *et al.*, Phys. Rev. B **66**, 020507 (2002); R. Shaikhaidarov *et al.*, *ibid.* **62**, R14649 (2000).
[3] J. J. A. Baselmans, T. T. Heikkilä, B. J. van Wees, and T. M. Klapwijk, Phys. Rev. Lett. **89**, 207002 (2002).
[4] A. F. Volkov, Phys. Rev. Lett. **74**, 4730 (1995).
[5] F. K. Wilhelm, G. Schön, and A. D. Zaikin, Phys. Rev. Lett. **81**, 1682 (1998).
[6] S.-K. Yip, Phys. Rev. B **58**, 5803 (1998).
[7] H. Pothier *et al.*, Phys. Rev. Lett. **79**, 3490 (1997).
[8] See W. Belzig *et al.*, Superlattices Microstruct. **25**, 1251 (1999), and references therein.
[9] T. T. Heikkilä, J. Särkkä, and F. K. Wilhelm, Phys. Rev. B **66**, 184513 (2002).
[10] K. D. Usadel, Phys. Rev. Lett. **25**, 507 (1970).
[11] D. R. Heslinga and T. M. Klapwijk, Phys. Rev. B **47**, 5157 (1993).
[12] At low control voltages there is a region of energies where $\mathcal{N}_1 = \mathcal{N}_2 = 0$. We assume that there the (otherwise weak) coupling to phonons makes the distributions at those energies equal to the equilibrium Fermi distribution. A more detailed discussion and another type of coupling is given in [13].
[13] J. P. Pekola *et al.*, Phys. Rev. Lett. **92**, 056804 (2004).
[14] A similar behavior was predicted by J. J. A. Baselmans, Ph. D. thesis, University of Groningen (2002).
[15] M. M. Leivo, J. P. Pekola, and D. V. Averin, Appl. Phys. Lett. **68**, 1996 (1996).
[16] A. Anthore, F. Pierre, H. Pothier, and D. Esteve, Phys. Rev. Lett. **90**, 076806 (2003).
[17] K. E. Nagaev, Phys. Rev. B **52**, 4740 (1995).
[18] B. L. Altshuler and A. G. Aronov, Zh. Eksp. Teor. Fiz. **75**, 1610 (1978) [Sov. Phys. JETP **48**, 812 (1978)].
[19] A. Kamenev and A. Andreev, Phys. Rev. B **60**, 2218 (1999).
[20] F. Giazotto *et al.*, Appl. Phys. Lett. **83**, 2877 (2003).
[21] This is straightforward assuming as typical parameters $\mathcal{R}_T = 10^3 \ \Omega$, $D = 0.02 \ \mathrm{m^2/s}$, and $\Delta_C = 200 \ \mu\mathrm{eV}$.
[22] In this calculation we chose to include depairing by a phenomenological but realistic parameter $\Gamma = 10^{-4}\Delta_C$ [13]. Its omission would lead to extremely higher $\mathbf{G}_I$ values. For $V_C \ll V_C^*$ and low temperature, Γ determines the differential resistance $R \approx \mathcal{R}_T \Delta_C / \Gamma$ of the SINIS line. Qualitatively, the large $\mathbf{G}_I$ stems from the fact $R \gg R_N$.